Int. J. Heat Mass Transfer. Vol. 31, No. 4, pp. 759–767, 1988
Printed in Great Britain

0017-9310/88 $3.00 + 0.00

Vortex instability of buoyancy-induced inclined boundary layer flow in a saturated porous medium

JIIN-YUH JANG and WEN-JENG CHANG
Department of Mechanical Engineering, National Cheng-Kung University, Tainan, Taiwan 70101, Republic of China

(*Received* 28 *May* 1987)

Abstract—A linear stability theory is used to analyse the vortex instability of buoyancy-induced boundary layer flow in a saturated porous medium adjacent to an inclined heated surface, where the wall temperature is a power function of the distance from the origin. In the main flow analysis, both the streamwise and normal component of the buoyancy force are retained in the momentum equations. Numerical results for surface heat transfer, the neutral stability curve, critical Rayleigh and wave numbers are presented for the angles of inclination ϕ from the horizontal in the range of 0 to 70°. It is found that as the angle of inclination from the horizontal increases, the heat transfer rate increases, whereas the susceptibility of the flow to the vortex mode of instability decreases. The present study provides new vortex instability results for small angles of inclination ($\phi \leqslant 30°$) and more accurate results for large angles of inclination ($\phi > 30°$) than the previous study by Hsu and Cheng (*ASME J. Heat Transfer* **101**, 660–665 (1979)), where the normal component of the buoyancy force in the main flow was neglected.

1. INTRODUCTION

THE BUOYANCY-induced motion of fluid through permeable material is an important mechanism of transport. Cheng and Chang [1] developed the similarity solutions for buoyancy-induced flow in a saturated porous medium adjacent to impermeable horizontal surfaces. In a subsequent paper, Hsu *et al.* [2] analysed the vortex mode of instability for a horizontal natural convection in a porous medium. Cheng and Minkowycz [3] presented a similarity analysis for a vertical flat plate embedded in a saturated porous medium.

For an inclined surface, the buoyancy force causing motion has a component in both the tangential and normal directions. This causes a pressure gradient across the boundary layer and leads to a theoretical analysis more complicated than that for a vertical or a horizontal surface. By neglecting the normal component of buoyancy force that induces the streamwise pressure gradient in the flow, Hsu and Cheng [4] showed that, in the main flow analysis, the boundary layer flow over an inclined heated plate can be approximated by the similarity solutions for a vertical plate, with the gravity component parallel to the inclined plate incorporated in the Rayleigh number; then the vortex instability was analysed by a local similarity method. Therefore, the main flow and instability results in ref. [4] are not valid for the angles of inclination from the vertical that are not small. This is because the normal component of the buoyancy force is responsible for the occurrence of the longitudinal vortices; and this component cannot be neglected when the angles of inclination from the vertical are large.

The purpose of this paper is to re-examine the main flow and vortex instability of free convection boundary layer flow over an inclined, upward-facing heated plate in a saturated porous medium, for the angles of inclination from the horizontal, ϕ, ranging from 0 to close to 90°. The wall temperature is a power function of the distance from the origin. Both the streamwise and normal components of the buoyancy force are retained in the momentum equations. This is in contrast to the previous analyses by Hsu and Cheng [4] that are generally valid only for $\phi > 45°$. Thus the present study covers the ranges of $0 < \phi \leqslant 45°$ in which no reliable stability results are available in the literature. The present resulting governing equations for the main flow do not admit similarity solutions. They are solved by using a suitable variable transformation and employing an efficient finite difference method similar to that described in Cebeci and Bradshaw [5]. The stability analysis is based on the linear theory. The disturbance quantities are assumed to be in the form of a stationary vortex roll that is periodic in the spanwise direction, with its amplitude function depending primarily on the normal coordinate and weakly on the streamwise coordinate. The resulting eigenvalue problem is solved using a variable step-size sixth-order Runge–Kutta integration routine incorporated with the Kaplan filtering technique [6] to maintain the linear independence of the two eigenfunctions. It should be noted that the corresponding problem for a viscous fluid was analysed by Chen and Tzuoo [7]. As might be expected, the qualitative result for a porous medium resembles that for a viscous fluid. However, there are some differences, notably those arising from the boundary conditions and the governing equations that differ in the two problems.

NOMENCLATURE

a	dimensional spanwise wave number
f	similarity stream function profile
F	dimensionless disturbance stream function amplitude
g	gravitational acceleration
k	dimensionless wave number, $ax/(Ra_x\cos\phi)^{1/3}$
k_1	dimensionless wave number, $ax/(Ra_x)^{1/3}$
K	Darcy permeability
Nu_x	local Nusselt number
P'	perturbation pressure
P	main flow pressure
Ra_x	local Rayleigh number, $\rho_\infty gK\beta(T_w-T_\infty)x/\mu\alpha$
t	time
T	temperature
T'	perturbation temperature
$\tilde{T}$	disturbance temperature amplitude
$\tilde{u}$	x-direction disturbance velocity amplitude
u, v, w	Darcy's velocity in x-, y-, z-direction
u', v', w'	axial, normal, and spanwise components of velocity disturbances
x, y, z	axial, normal, and spanwise coordinates.

Greek symbols

α	effective thermal diffusivity
β	coefficient of thermal expansion
δ_t	thermal boundary layer thickness
η	similarity variable, $y(Ra_x\cos\phi)^{1/3}/x$
θ	dimensionless temperature, $(T-T_\infty)/(T_w-T_\infty)$
Θ	dimensionless disturbance temperature amplitude
λ	volumetric heat capacity of the saturated porous medium to that of the fluid
μ	viscosity
ρ	density
σ	temporal growth constant
υ	kinematic viscosity
ϕ	angle of inclination measured from the horizontal
ψ	stream function
ψ'	disturbance stream function
$\tilde{\psi}$	disturbance stream function amplitude.

Subscripts

w	condition at the wall
∞	condition at the free stream.

Superscripts

*	critical condition
~	amplitude function for disturbance.

2. ANALYSIS

2.1. *The main flow*

Consider an inclined impermeable surface (T_w) embedded in a porous medium (T_∞) as shown in Fig. 1, where x represents the distance along the plate from its leading edge, and y represents the distance normal to the surface. The wall temperature is assumed to be a power function of x, i.e. $T_w = T_\infty + Ax^m$, where A is a constant. The angle of inclination, ϕ, is measured from the horizontal. The following conventional assumptions simplify the analysis.

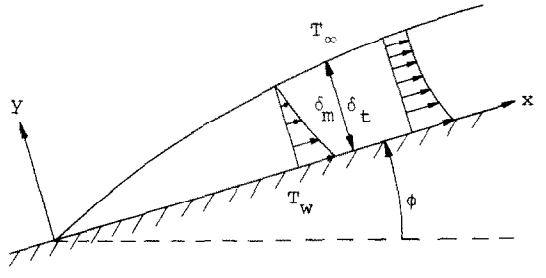

FIG. 1. Coordinate system.

(1) The physical properties are considered to be constant, except for the density term that is associated with the body force.

(2) Flow is sufficiently slow that the convecting fluid and the porous matrix are in local thermodynamic equilibrium.

(3) Darcy's law and the Boussinesq approximation are employed.

With these assumptions, the governing equations are given by

$$\frac{\partial u}{\partial x}+\frac{\partial v}{\partial y}=0 \tag{1}$$

$$u=-\frac{K}{\mu}\left(\frac{\partial P}{\partial x}+\rho g\sin\phi\right) \tag{2}$$

$$v=-\frac{K}{\mu}\left(\frac{\partial P}{\partial y}+\rho g\cos\phi\right) \tag{3}$$

$$u\frac{\partial T}{\partial x}+v\frac{\partial T}{\partial y}=\alpha\left(\frac{\partial^2 T}{\partial x^2}+\frac{\partial^2 T}{\partial y^2}\right) \tag{4}$$

$$\rho=\rho_\infty(1-\beta(T-T_\infty)) \tag{5}$$

where K is the permeability of the saturated porous medium; β the coefficient for thermal expansions; and α represents the equivalent thermal diffusivity. The other symbols are defined in the nomenclature.

The pressure terms appearing in equations (2) and (3) can be eliminated through cross-differentiation. By applying the boundary layer assumptions ($\partial/\partial x \ll \partial/\partial y, v \ll u$) and introducing the stream function ψ which automatically satisfies equation (1), equations (1)–(5) become

$$\frac{\partial^2\psi}{\partial y^2} = \frac{\rho_\infty g\beta K}{\mu}\left(\frac{\partial T}{\partial y}\sin\phi - \frac{\partial T}{\partial x}\cos\phi\right) \tag{6}$$

$$\frac{\partial\psi}{\partial y}\frac{\partial T}{\partial x} - \frac{\partial\psi}{\partial x}\frac{\partial T}{\partial y} = \alpha\frac{\partial^2 T}{\partial y^2}. \tag{7}$$

The boundary conditions for this problem are

$$\begin{aligned} &\text{at } y = 0 \quad \frac{\partial\psi}{\partial x} = 0; \quad T_w = T_\infty + AX^m \\ &\text{as } y \to \infty \quad \frac{\partial\psi}{\partial y} \to 0; \quad T \to T_\infty \\ &\text{at } x = 0 \quad \frac{\partial\psi}{\partial y} = 0; \quad T = T_\infty. \end{aligned} \tag{8}$$

The following dimensionless variables are introduced:

$$\begin{aligned} \xi(x) &= (Ra_x\cos\phi)^{1/3}\tan\phi \\ \eta(x,y) &= y(Ra_x\cos\phi)^{1/3}/x \\ f(\xi,\eta) &= \frac{\psi(x,y)}{\alpha(Ra_x\cos\phi)^{1/3}} \\ \theta(\xi,\eta) &= (T-T_\infty)/(T_w-T_\infty) \end{aligned} \tag{9}$$

where

$$Ra_x = \rho_\infty gK\beta(T_w - T_\infty)x/\mu\alpha$$

is the modified local Rayleigh number. Then, equations (6) and (7) become

$$f'' + m\theta + \frac{(m-2)}{3}\eta\theta' = \xi\left(\theta' - \frac{(m+1)}{3}\frac{\partial\theta}{\partial\xi}\right) \tag{10}$$

$$\theta'' + \frac{(m+1)}{3}f\theta' - mf'\theta = \frac{(m+1)}{3}\xi\left(f'\frac{\partial\theta}{\partial\xi} - \theta'\frac{\partial f}{\partial\xi}\right) \tag{11}$$

with boundary conditions

$$f(\xi,0) = 0, \quad \theta(\xi,0) = 1, \quad f'(\xi,\infty) = 0, \quad \theta(\xi,\infty) = 0. \tag{12}$$

In the foregoing equations, the primes denote partial differentiation with respect to η. Equations (10)–(12) are valid for all angles except $\phi = \pi/2$ because $\xi \to \infty$ as $\phi \to \pi/2$. They reduce to those equations for flow over a horizontal flat plate [1] when $\xi = 0$.

In terms of new variables, it can be shown that the velocity components and local Nusselt number are given by

$$\begin{aligned} u(x,y) &= \left[\frac{\alpha(Ra_x\cos\phi)^{2/3}}{x}\right]f'(\xi,\eta) \\ v(x,y) &= -\frac{\alpha(Ra_x\cos\phi)^{1/3}}{3x} \\ &\quad\times\left[(m+1)f + (m-2)\eta f' + (m+1)\xi\frac{\partial f}{\partial\xi}\right] \\ Nu_x(Ra_x\cos\phi)^{-1/3} &= -\theta'(\xi,0). \end{aligned} \tag{13}$$

2.2. *The disturbance flow*

The standard method of linear stability theory in which the instantaneous values of the velocity, pressure and temperature are perturbed by small amplitude disturbances and the mean flow quantities are subtracted, with terms higher than first order in disturbance quantities being neglected result in the disturbance equations. Then, we get

$$\frac{\partial u'}{\partial x} + \frac{\partial v'}{\partial y} + \frac{\partial w'}{\partial z} = 0 \tag{14}$$

$$u' = -\frac{K}{\mu}\left[\frac{\partial P'}{\partial x} - \rho_\infty g\beta\sin\phi\cdot T'\right] \tag{15}$$

$$v' = -\frac{K}{\mu}\left[\frac{\partial P'}{\partial y} - \rho_\infty g\beta\cos\phi\cdot T'\right] \tag{16}$$

$$w' = -\frac{K}{\mu}\frac{\partial P'}{\partial z} \tag{17}$$

$$\lambda\frac{\partial T'}{\partial t} + \bar{u}\frac{\partial T'}{\partial x} + u'\frac{\partial\bar{T}}{\partial x} + \bar{v}\frac{\partial T'}{\partial y} + v'\frac{\partial\bar{T}}{\partial y} = \alpha\left(\frac{\partial^2 T'}{\partial x^2} + \frac{\partial^2 T'}{\partial y^2} + \frac{\partial^2 T'}{\partial z^2}\right) \tag{18}$$

where the barred and primed quantities signify the mean flow and disturbance components, and λ is the volumetric heat capacity of the saturated porous medium to that of the fluid.

Following the method of order-of-magnitude analysis prescribed in detail by Hsu and Cheng [4], the terms $\partial u'/\partial x$, $\partial^2 T'/\partial x^2$ in equations (14) and (18) can be neglected. The omission of $\partial u'/\partial x$ in equation (14) implies the existence of a disturbance stream function ψ' such that

$$w' = \frac{\partial\psi'}{\partial y}, \quad v' = -\frac{\partial\psi'}{\partial z}. \tag{19}$$

Eliminating P' from equations (15)–(17), and with the aid of equations (19), leads to

$$\frac{\partial u'}{\partial z} - \frac{\partial^2\psi'}{\partial x\,\partial y} = \frac{\rho_\infty gK\beta}{\mu}\frac{\partial T'}{\partial z}\sin\phi \tag{20}$$

$$\frac{\partial^2\psi'}{\partial y^2} + \frac{\partial^2\psi'}{\partial z^2} = -\frac{\rho_\infty gK\beta}{\mu}\frac{\partial T'}{\partial z}\cos\phi \tag{21}$$

$$\lambda\frac{\partial T'}{\partial t}+\bar{u}\frac{\partial T'}{\partial x}+u'\frac{\partial \bar{T}}{\partial x}+\bar{v}\frac{\partial T'}{\partial y}-\frac{\partial \psi'}{\partial z}\frac{\partial \bar{T}}{\partial y}=\alpha\left(\frac{\partial^2 T'}{\partial y^2}+\frac{\partial^2 T'}{\partial z^2}\right). \quad (22)$$

As in Hsu and Cheng [4], we assume that the three-dimensional disturbances are of the form

$$(\psi', u', T') = [\tilde{\psi}(x,y), \tilde{u}(x,y), \tilde{T}(x,y)] \times \exp(\mathrm{i}az+\sigma t+\gamma(x)) \quad (23)$$

where a is the spanwise periodic wave number, σ is the temporal growth factor while

$$\gamma(x) = \int \alpha_i(x)\,\mathrm{d}x$$

with $\alpha_i(x)$ denoting the spatial growth factor. Substituting equation (23) into equations (20)–(22) and setting $\sigma = \alpha_i = 0$ for neutral stability yields

$$\mathrm{i}a\tilde{u}-\frac{\partial^2\tilde{\psi}}{\partial x\,\partial y}=\frac{\mathrm{i}\rho_\infty gK\beta a}{\mu}\sin\phi\cdot\tilde{T} \quad (24)$$

$$\frac{\partial^2\tilde{\psi}}{\partial y^2}-a^2\tilde{\psi}=-\frac{\mathrm{i}\rho_\infty gK\beta a}{\mu}\cos\phi\cdot\tilde{T} \quad (25)$$

$$\alpha\left(\frac{\partial^2\tilde{T}}{\partial y^2}-a^2\tilde{T}\right)=\bar{u}\frac{\partial\tilde{T}}{\partial x}+\bar{v}\frac{\partial\tilde{T}}{\partial y}+\tilde{u}\frac{\partial\bar{T}}{\partial x}-\mathrm{i}a\tilde{\psi}\frac{\partial\bar{T}}{\partial y}. \quad (26)$$

Equations (24)–(26) are solved based on the local similarity approximations [4], wherein the disturbances are assumed to have weak dependence in the streamwise direction (i.e. $\partial/\partial x \ll \partial/\partial y$).

We let

$$F(\eta)=\frac{\tilde{\psi}}{\mathrm{i}\alpha(Ra_x\cos\phi)^{1/3}},\quad \Theta(\eta)=\tilde{T}/Ax^m,\quad k=ax/(Ra_x\cos\phi)^{1/3}. \quad (27)$$

One gets the following system of equations for the local similarity approximations:

$$\tilde{u}=\frac{\alpha(Ra_x\cos\phi)^{2/3}}{a}\left(\frac{m-2}{3x^2}\eta F''+\frac{2m-1}{3x^2}F'\right)+\frac{\rho_\infty Kg\beta\sin\phi}{\mu}Ax^m\Theta \quad (28)$$

$$F''-k^2F=-k(Ra_x\cos\phi)^{1/3}\Theta \quad (29)$$

$$\Theta''-k^2\Theta=(mf')\Theta-\left(\frac{m+1}{3}f+\frac{m+1}{3}\xi\frac{\partial f}{\partial\xi}\right)\Theta'+\left(m\theta+\frac{m+1}{3}\xi\frac{\partial\theta}{\partial\xi}+\frac{m-2}{3}\eta\theta'\right)\frac{x}{\alpha(Ra_x\cos\phi)^{2/3}}\tilde{u}+[k(Ra_x\cos\phi)^{1/3}\theta']F. \quad (30)$$

Then, the substitution of $\tilde{u}$ and Θ from equations (28) and (29) into equation (30) yields

$$(\mathrm{D}^2-k^2)^2F-\left(mf''+m\xi\theta+\frac{m+1}{3}\xi^2\frac{\partial\theta}{\partial\xi}+\frac{m-2}{3}\eta\xi\theta'\right)(\mathrm{D}^2-k^2)F+\left(\frac{m+1}{3}f+\frac{m+1}{3}\xi\frac{\partial f}{\partial\xi}\right)\mathrm{D}\times(\mathrm{D}^2-k^2)F+\left(m\theta+\frac{m+1}{3}\xi\frac{\partial\theta}{\partial\xi}+\frac{m-2}{3}\eta\theta'\right)\times\left(\frac{m-2}{3}\eta F''+\frac{2m-1}{3}F'\right)+k^2(Ra_x\cos\phi)^{2/3}\theta'F=0 \quad (31)$$

with the boundary conditions

$$F(0)=\mathrm{D}^2F(0)=F(\infty)=\mathrm{D}^2F(\infty)=0 \quad (32)$$

where D^n stands for $\mathrm{d}n/\mathrm{d}\eta$. Equation (31) along with its boundary condition, equation (32), constitutes a fourth-order system of linear ordinary differential equations for the disturbance amplitude distributions $F(\eta)$. For fixed m and ϕ, the solution F is an eigenfunction for the eigenvalues Ra_x and k.

3. NUMERICAL METHOD OF SOLUTION

Equations (10)–(12) for the base flow were solved by an implicit finite difference scheme similar to, but modified from that described in ref. [5]. Its details are omitted here. In the stability calculations, the disturbance equations are solved by separately integrating two linearly independent integrals. The full equations may be written as the sum of two linearly independent solutions $F(\eta) = F_1 + BF_2$. The two independent integrals F_1 and F_2 may be chosen so that their asymptotic solutions are

$$F1=\mathrm{e}^{-k\eta},\quad F2=\mathrm{e}^{-A\eta} \quad (33)$$

where

$$A=\frac{m+1}{6}\left(f+\xi\frac{\partial f}{\partial\xi}\right)+\left\{\left[\frac{m+1}{6}\left(f+\xi\frac{\partial f}{\partial\xi}\right)\right]^2+\left[\left(m\phi+\frac{m+1}{3}\xi\frac{\partial\theta}{\partial\xi}+\frac{m-2}{3}\eta\theta'\right)\xi\right]+k^2\right\}^{1/2}.$$

Equation (31) with boundary conditions, equation (32), are then solved as follows. For specified m, ϕ and Ra_x, k is guessed. Using equations (33) as starting values, the two integrals are integrated separately from the outer edge of the boundary layer to the wall using a sixth-order Runge–Kutta variable size integrating routine incorporated with the Kaplan filtering technique [6] to maintain the linear independence of the eigenfunctions. The required input of the base flow to the disturbance equations is calculated, as necessary, by linear interpolation of the stored base flow. From the values of the integrals at the wall, B is determined using the boundary conditions $F(0) = 0$. The second boundary condition

$D^2F(0) = 0$ is satisfied only for the appropriate value of the eigenvalue k. A Taylor series expansion of the initial guess of k provides a correction scheme for the initial guess of k. Iterations continue until the second boundary condition is sufficiently close to zero ($< 10^{-6}$, typically).

4. RESULTS AND DISCUSSIONS

Figure 2 shows the effects of the inclination parameter $\xi = (Ra_x \cos\phi)^{1/3} \tan\phi$ on the dimensionless tangential velocity profile f' across the boundary layer for $m = 0$. It is seen that, as would be expected, the dimensionless tangential velocity increases with increasing value of ξ; that is, the tangential velocity increases with increasing value of Ra_x for a given angle ϕ or increases with increasing inclination angle ϕ for a given Rayleigh number Ra_x. The dashed lines represent the similarity solutions for an equivalent vertical plate [4], where the normal component of the buoyancy force is neglected in the main flow. It is noted that the equivalent vertical plate solutions have been transformed to present (ξ, η) coordinates for easy comparison with our non-similar solutions. Note that large calculated differences from the equivalent vertical plate results are apparent for $\xi \leqslant 3$. That is, the discrepancy is getting larger for small angles of inclination.

Figure 3 shows the effects of the inclination parameter ξ on the dimensionless temperature profiles across the boundary layer for $m = 0$. As can be seen from this figure, as ξ increases, the temperature boundary layer thickness decreases. Numerical solutions of the local Nusselt number for selected values of m are shown in Fig. 4 for various values of inclination parameter ξ. As expected, the local Nusselt number increases as ξ increases. It is also revealed that the equivalent vertical results underestimate the heat transfer rate.

From Figs. 2–4, the equivalent vertical solutions show considerably good agreement with our present results for $\xi \geqslant 7$; however as ξ decreases to zero, the equivalent vertical solutions are seen to deviate further from the present results. This is because as ξ decreases, the normal component of gravity is more pronounced. Thus the equivalent vertical plate results for small values of ξ are not accurate. The solutions of Cheng and Chang [1] for a horizontal plate (i.e. $\xi = \phi = 0$) are also included in Figs. 2–4. It is shown that our present results are in excellent agreement with ref. [1].

Figure 5 shows the neutral stability curves for selected values of ϕ (0, 5, 20, 30, 50 and 70°) at $m = 0$. It is seen that as the inclination angle ϕ increases, the neutral stability curves shift to higher Rayleigh number and higher wave number, indicating a stabilization of the flow to the vortex instability. The dashed lines denote the stability analysis from Hsu and Cheng [4], where the normal component of the buoyancy force

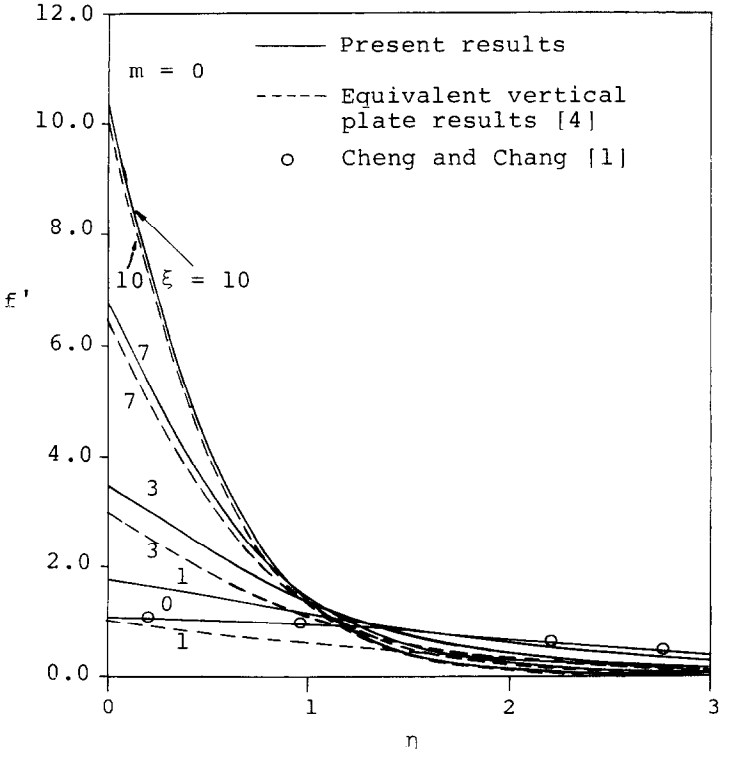

FIG. 2. The variations of the tangential velocity component across the boundary layer for various ξ. Dashed curves represent the equivalent vertical plate results [4].

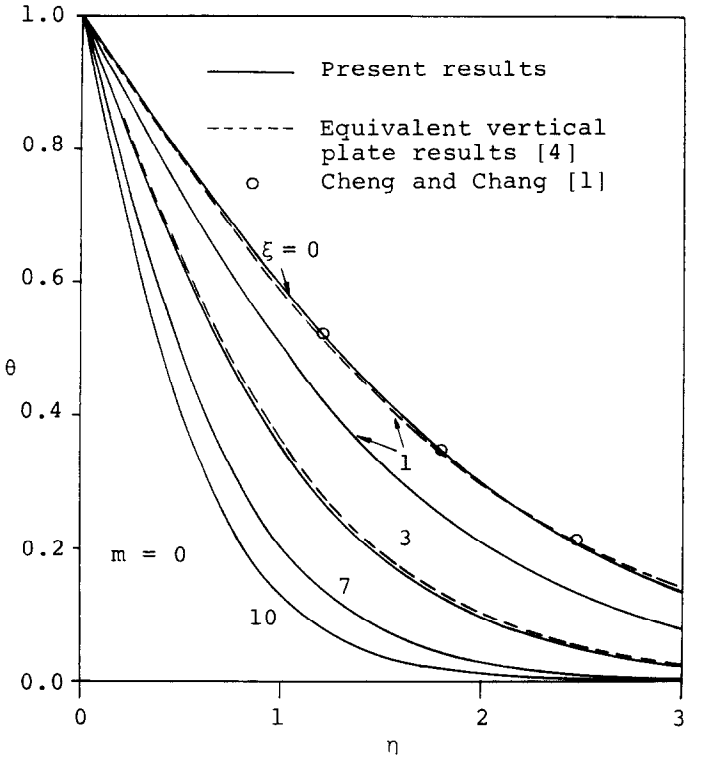

FIG. 3. The temperature profiles across the boundary layer for various ξ. Dashed curves represent the equivalent vertical plate results [4].

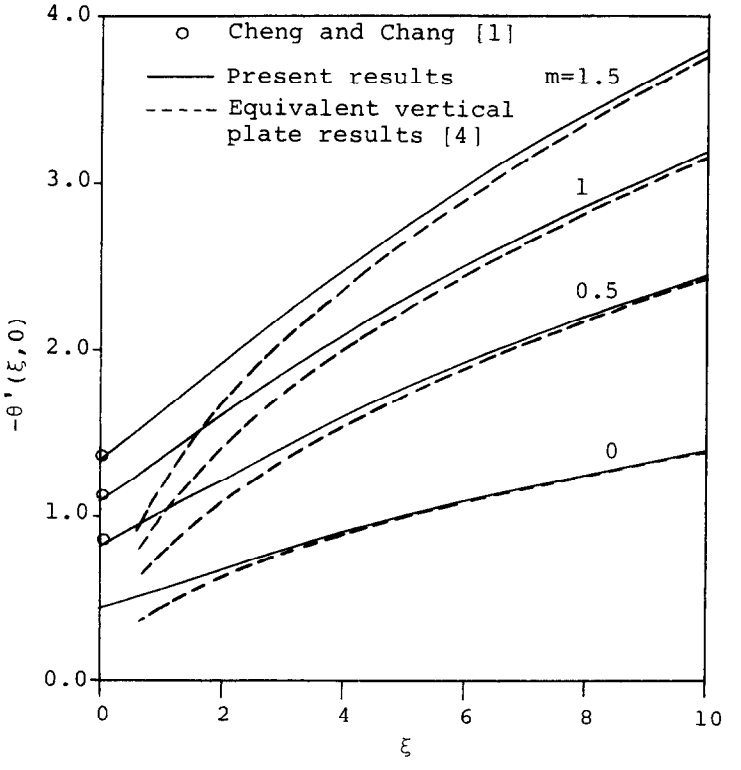

FIG. 4. The local Nusselt number vs ξ for selected values of m. Dashed curves represent the equivalent vertical plate results [4].

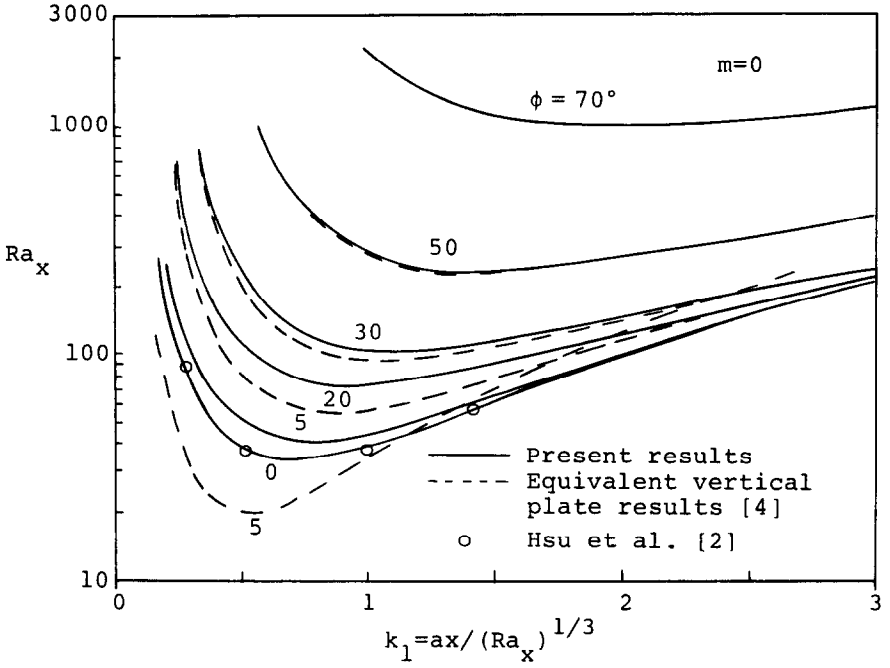

FIG. 5. Neutral stability curves for selected values of inclination angles ϕ.

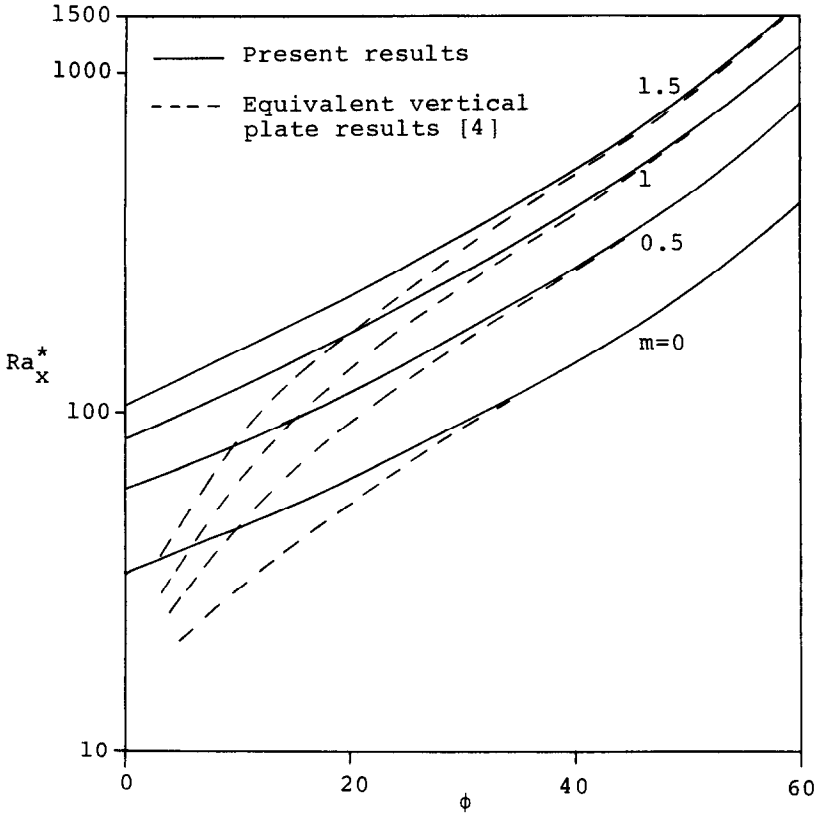

FIG. 6. Critical Rayleigh number vs ϕ for selected values of m.

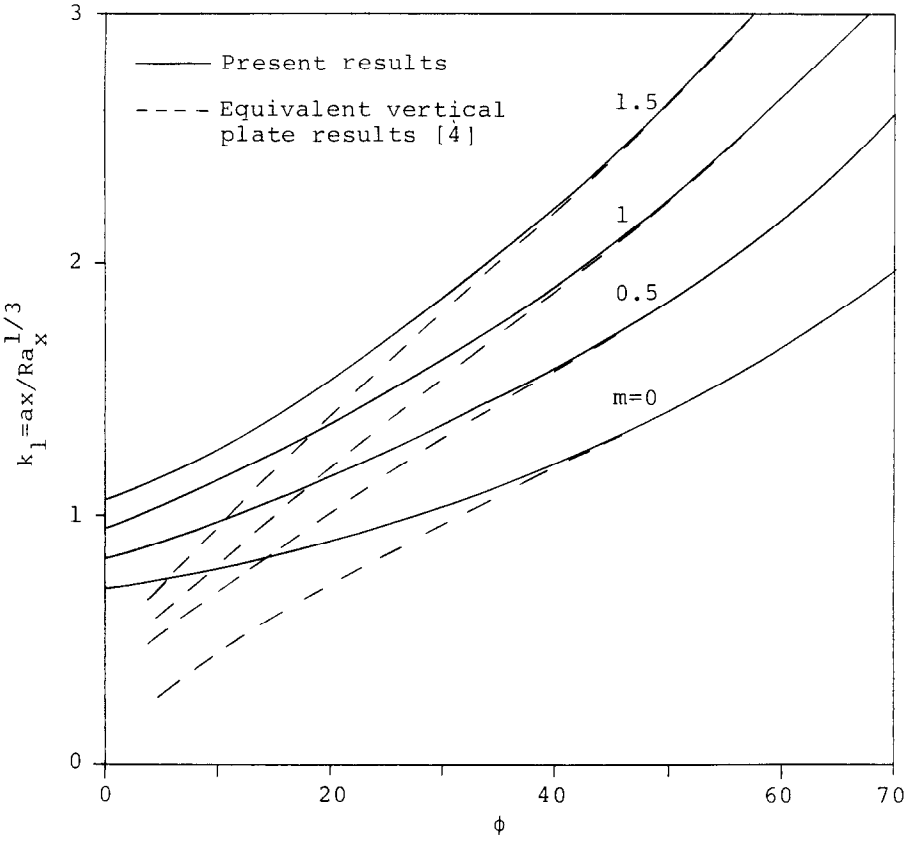

FIG. 7. Dimensionless critical wave number vs ϕ for selected values of m.

was not included in the main flow. It is shown that as ϕ decreases the two sets of results deviate more. On the other hand, as $\phi > 30°$, these two sets of solutions differ very little whether the normal component of the buoyancy force is included in the main flow or not. This is due to the fact that for large ϕ the normal component of the buoyancy force is small, so it can be neglected. For $\phi = 0$ ($\xi = 0$), our present results are in good agreement with those of Hsu *et al.* [2].

The critical Rayleigh number and wave number, which marks the onset of longitudinal vortices, are plotted as a function of inclination angle ϕ in Figs. 6 and 7, respectively, for $m = 0$, 0.5, 1 and 1.5. It is seen that the critical Rayleigh number is a rather strong function of m. The larger the value of m is, the flow is more stable for the vortex mode of instability. This is because as m increases, the streamwise driving force (i.e. the terms $\tilde{u}(\partial\tilde{T}/\partial x)$ and $\tilde{u}(\partial\bar{T}/\partial x)$ in equation (26)) increases. Consequently, the flow is more stable. It is apparent from Fig. 7 that the critical wave number increases as ϕ increases. Also appearing in these two figures are dashed lines representing the stability results obtained by Hsu and Cheng [4], where the normal component of the buoyancy force is neglected. It is seen that the equivalent vertical plate assumption leads to significant errors in the stability results as ϕ decreases from 30° down to the horizontal orientation. It is also shown that as m increases, the deviation in the two sets of results is seen to become larger.

5. CONCLUSIONS

A linear stability analysis is made to re-examine the buoyancy-induced flow in a porous medium adjacent to an inclined heated surface. The results show that both the critical Rayleigh number and wave number are increased as the plate inclination is increased from the horizontal. The stability analysis based on the equivalent vertical plate assumptions in the main flow is found to be inadequate as the angle of inclination from the horizontal is less than 30°. It is also found that as the index of power law m increases, the flow becomes less susceptible to the vortex instability, and the discrepancy of the heat transfer rate, critical Rayleigh and wave numbers between our present results and the equivalent vertical plate results become larger.

REFERENCES

1. P. Cheng and I. D. Chang, Buoyancy induced flows in a saturated porous medium adjacent to impermeable horizontal surfaces, *Int. J. Heat Mass Transfer* **19**, 1267–1272 (1976).
2. C. T. Hsu, P. Cheng and G. M. Homsy, Instability of free

convection flow over a horizontal impermeable surface in a porous medium, *Int. J. Heat Mass Transfer* **21,** 1221–1228 (1978).
3. P. Cheng and W. J. Minkowycz, Free convection about a vertical flat plate embedded in a porous medium with application to heat transfer from a dike, *J. Geophys. Res.* **82,** 2040–2044 (1977).
4. C. T. Hsu and P. Cheng, Vortex instability in buoyancy-induced flow over inclined heated surfaces in a porous media, *ASME J. Heat Transfer* **101,** 660–665 (1979).
5. T. Cebeci and P. Bradshaw, *Physical and Computational Aspects of Convective Heat Transfer*, Chap. 13. Springer, New York (1984).
6. R. E. Kaplan, The stability of laminar incompressible boundary layers in the presence of complaint boundaries, M.I.T. Aero-elastic and Structures Research Laboratory, ASRL-TR 116-1 (1964).
7. T. S. Chen and L. Tzuoo, Vortex instability of free convection flow over horizontal and inclined surfaces, *ASME J. Heat Transfer* **104,** 637–643 (1982).

INSTABILITE TOURBILLONNAIRE D'UN ECOULEMENT INCLINE DE COUCHE LIMITE INDUIT PAR PESANTEUR DANS UN MILIEU POREUX SATURE

Résumé—Une théorie linéaire de stabilité est utilisée pour analyser l'instabilité tourbillonnaire de l'écoulement de couche limite induit par pesanteur dans un milieu poreux saturé adjacent à une surface chaude inclinée, où la température pariétale est une fonction puissance de la distance à l'origine. Dans l'analyse de l'écoulement principal, on retient dans les équations de quantité de mouvement les composantes normale et longitudinale de la force de pesanteur. Les résultats numériques pour le transfert thermique à la surface, la courbe de stabilité neutre, les nombres de Rayleigh critiques et les nombres d'ondes, sont présentés pour un domaine d'angle d'inclinaison ϕ à partir de l'horizontale compris entre 0 et 70°. On trouve que lorsque l'angle d'inclinaison augmente, le flux thermique croît tandis que la susceptibilité de l'écoulement au mode tourbillonnaire d'instabilité diminue. La présente étude fournit des résultats nouveaux pour les petits angles ($\phi \leqslant 30°$) et des résultats pour des grands angles ($\phi > 30°$) plus précis que dans l'étude de Hsu et Cheng (*ASME J. Heat Transfer* **101,** 660–665 (1979)) qui néglige la composante normale de la force de pesanteur dans l'écoulement principal.

WIRBELINSTABILITÄT IN EINER AUFTRIEBSINDUZIERTEN GENEIGTEN GRENZSCHICHTSTRÖMUNG IN EINEM GESÄTTIGTEN PORÖSEN MEDIUM

Zusammenfassung—Es wird eine lineare Stabilitätstheorie verwendet, um die Wirbelinstabilität in einer auftriebsinduzierten Grenzschichtströmung an einer geneigten, beheizten Oberfläche in einem gesättigten porösen Medium zu bestimmen. Die Wandtemperatur ist eine Potenzfunktion der Entfernung vom Zuströmpunkt. Zur Bestimmung der Hauptströmung sind die Komponenten der Auftriebskraft in Strömungsrichtung und senkrecht dazu in der Impulsgleichung enthalten. Die numerischen Berechnungen des Wärmeübergangskoeffizienten, der neutralen Stabilitätskurve und der kritischen Rayleigh- und der Wellenzahl sind in Abhängigkeit vom Neigungswinkel ϕ zur Horizontalen im Bereich von 0° bis 70° dargestellt. Es zeigte sich, daß für steigende Neigungswinkel der Wärmeübergang zunimmt, wohingegen die Anfälligkeit der Strömung gegen Wirbelinstabilität sinkt. Die Untersuchung liefert für kleine Neigungswinkel ($\phi \leqslant 30°$) neue Ergebnisse für die Wirbelinstabilität. Für große Neigungswinkel ($\phi > 30°$) werden genauere Ergebnisse erreicht als bei Hsu und Cheng (*ASME J. Heat Transfer* **101,** 660–665 (1979)), die den Einfluß der Normalenkomponente der Auftriebskraft auf die Hauptströmung vernachlässigt haben.

ВИХРЕВАЯ НЕУСТОЙЧИВОСТЬ ВЫЗЫВАЕМОГО ПОДЪЕМНОЙ СИЛОЙ НАКЛОННОГО ТЕЧЕНИЯ В ПОГРАНИЧНОМ СЛОЕ В НАСЫЩЕННОЙ ЖИДКОСТЬЮ ПОРИСТОЙ СРЕДЕ

Аннотация—На основе линейной теории устойчивости анализируется вихревая неустойчивость вызываемого подъемной силой течения в пограничном слое в насыщенной жидкостью пористой среде, прилегающей к наклонной нагреваемой поверхности, где температура стенки является степенной функцией расстояния от начальной точки. Для анализа течения вне пограничного слоя в уравнении количества движения учтена как компонента подъемной силы, действующей в направлении потока, так и компонента, направленная по нормали к потоку. Приведены численные результаты по теплообмену поверхности, кривая нейтральной устойчивости, критическое число Рэлея и волновое число для углов наклона поверхности ϕ к горизонтали от 0 до 70°. Показано, что по мере увеличения угла наклона интенсивность теплообмена возрастает, в то время как влияние режима вихревой неустойчивости на течение уменьшается. Получены новые данные по вихревой неустойчивости при небольших углах наклона ($\phi \leqslant 30°$) и учтены результаты, полученные ранее Хсу и Ченгом при углах наклона $\phi > 30°$ (*Теплопередача* том **101,** стр. 660–665 (1979)) в пренебрежении нормальной компонентой подъемной силы основного потока.